2024

Parametric Study of the Effect of Increased Magnetic Field Exposure on Microalgae *Chlorella vulgaris* Growth and Bioactive Compound Production

Sharanabasaweshwara Asundi
Old Dominion University

Sanurag Rout
University of Minnesota - Twin Cities

Simone Stephen
Old Dominion University

Sanghamitra Khandual
The Center for Research and Assistance in Technology and Design of the State of Jalisco, AC (CIATEJ)

Sandipan Dutta
Old Dominion University

See next page for additional authors

Original Publication Citation

Asundi, S., Rout, S., Stephen, S., Khandual, S., Dutta, S., & Kumar, S. (2024). Parametric study of the effect of increased magnetic field exposure on microalgae *Chlorella vulgaris* growth and bioactive compound production. *Phycology*, *4*(2), 314-329. https://doi.org/10.3390/phycology4020016

phycology

MDPI

Article

Parametric Study of the Effect of Increased Magnetic Field Exposure on Microalgae *Chlorella vulgaris* Growth and Bioactive Compound Production

Sharanabasaweshwara Asundi [1,*], Sanurag Rout [2], Simone Stephen [1], Sanghamitra Khandual [3], Sandipan Dutta [4] and Sandeep Kumar [5]

[1] Department of Mechanical and Aerospace Engineering, Old Dominion University, Norfolk, VA 23529, USA; sstep008@odu.edu
[2] Department of Aerospace Engineering and Mechanics, University of Minnesota Twin Cities, Minneapolis, MN 55455, USA; sanurag997@gmail.com
[3] The Center for Research and Assistance in Technology and Design of the State of Jalisco, AC (CIATEJ), Guadalajara 44680, Mexico; mita@ciatej.mx
[4] Department of Mathematics & Statistics, Old Dominion University, Norfolk, VA 23529, USA; s1dutta@odu.edu
[5] Department of Civil & Environmental Engineering, Old Dominion University, Norfolk, VA 23529, USA; skumar@odu.edu
* Correspondence: sasundi@odu.edu; Tel.: +1-757-683-3752

Simple Summary: Simple Summary: This study aims to contribute to the fundamental understanding of the effect of increased magnetic field exposure (MFE) on the growth and production of *Chlorella (C.) vulgaris*, a species of green microalga. To study the effects of an increased MFE, the magnetic field typically experienced by life on Earth was amplified by an order of magnitude. In this study, six treatments of *C. vulgaris* with two repetitions for each treatment were exposed to a magnetic field of 5 Gauss (500 μT) about each axis, which was generated in a precision state-of-the-art calibrated Helmholtz cage. The treatments and the control were characterized by the duration of exposure, which was varied from 0 min to 120 min with a step increment of 20 min. The treatments were repeated for six days and twelve days in two separate experiments. For the parametric study of the outcomes, the treated species were analyzed for overall growth, protein, and beta-carotene content. It was largely observed that the increased MFE had a significant impact on the overall growth and to a lesser extent on the protein and beta-carotene production.

Abstract: This parametric study aimed to analyze the effects of increased magnetic field exposure (MFE) on the growth and production of the bioactive compounds of *Chlorella (C.) vulgaris*. With the intent of studying the effect of an increased MFE, the magnetic field typically experienced by life on Earth was amplified by an order of magnitude. In the increased-MFE environment, six treatments of *C. vulgaris* with two repetitions for each treatment were exposed to a magnetic field of 5 Gauss (500 μT) about each axis, which was generated in a state-of-the-art Helmholtz cage. The treatments and the control were characterized by the duration of exposure, which was varied from 0 min to 120 min with a step increment of 20 min. The treatments were repeated for six days (TR1) and twelve days (TR2) in two separate experiments. From the first day of the treatment, the specimens in both the experiments were propagated for twenty-one days. For parametric analysis, the overall growth, protein, and beta-carotene content were measured every three days for twenty-one days. For TR1 in general, the samples treated with the increased MFE demonstrated a higher growth rate than the control. Specifically, for the specimen treated with 40 min of the increased MFE, the growth on the 21st day was measured to be 38% higher than the control. For the specimen treated with 120 min of the increased MFE, the protein content on the 15th day was measured to be 15.6% higher than the control. For the specimen treated with 40 min of the increased MFE, the beta-carotene content on the 15th day was measured to be 20.4% higher than the control. For TR2 in general, the results were inferior compared to TR1 but showed higher production than the control specimen. Specifically, for the specimen treated with 80 min of the increased MFE, the protein content on the 21st day was

check for updates

Citation: Asundi, S.; Rout, S.; Stephen, S.; Khandual, S.; Dutta, S.; Kumar, S. Parametric Study of the Effect of Increased Magnetic Field Exposure on Microalgae *Chlorella vulgaris* Growth and Bioactive Compound Production. *Phycology* **2024**, *4*, 314–329. https://doi.org/10.3390/phycology4020016

Academic Editor: Adele Cutignano

Received: 26 December 2023
Revised: 15 May 2024
Accepted: 26 May 2024
Published: 6 June 2024

measured to be 4.3% higher than the control. For the specimen treated with 100 min of the increased MFE, the beta-carotene content on the 15th day was measured to be 17.1% higher than the control. For the specimen treated with 100 min of the increased MFE, the growth on the 21st day was measured to be 5% higher than the control. Overall, the treated specimens in TR1 exhibited significantly higher production compared to the control specimen. The treated specimen in TR2 demonstrated some adverse impacts, but still exhibited higher production compared to the control specimen.

Keywords: beta-carotene; *Chlorella vulgaris*; Helmholtz cage; magnetic field exposure; optical density growth; protein; space biology

1. Introduction

Magnetic fields are common throughout the solar system and extrasolar systems. The Sun, Mercury, Earth, the giant planets, and the Jovian satellite Ganymede [1] have intrinsic magnetic fields. It has been observed that many extrasolar planets have variable magnetic fields [2]. Planetary magnetic fields result from a dynamo action [3] and are linked to the planets' internal dynamics. According to their magnetic fields, the planets in our solar system are classified into two types. The type-I planets such as Venus, Mars, and Pluto (also the Moon) have a weak global magnetic field. These planets either lack or have a very weak magnetosphere [4]. However, the type-II planets such as Mercury, Earth, Jupiter, Saturn, Uranus, and Neptune have strong global magnetic fields. The magnetism of planets has intrigued scientists for years. The Earth, itself, generates a "planetary scale magnetic field of 0.25–0.65 Gauss in the conductive and convective outer core" [5]. The magnetic field is known to have characteristics and parameters that shelter the Earth from the damaging effects of solar wind plasmas [6]. The magnetic field around the Earth acts as a shield for the energetic cosmic radiation deflecting most of the harmful radiation away from Earth. The knowledge of Earth's magnetic field has led to scientific inventions such as the compass and the understanding that it changes over time [7].

Several studies have demonstrated that magnetic field exposure (MFE) can have varying effects on biological life. An increased MFE is that which is not typically experienced by life on Earth and is representative of the MFE experienced in space and/or the surface of planetary bodies. Some recent studies report that exposure to static magnetic fields induced oxidative stress in *Scenedesmus* and *Nannochloropsis* and significantly increased the production of antioxidant pigments and enzymes [8]. Some other studies have reported growth in the production of microorganisms and increased biomass, pigments, carbohydrate, and protein concentrations [9,10]. Tu et al. [9] concluded that a 100 mT MFE increased the growth and oxygen production of *Scenedesmus obliquus*. Small et al. [10] demonstrated that a 10 mT MFE increased the biomass and nutritional value of *Chlorella (C.) kessleri* microalgae. These results show that the magnitude or intensity of the MFE can have a varying effect on microorganisms. Yang et al. [11] demonstrated that magnetic treatment of *C. vulgaris* could result in increased production and cause changes in the biological cells and movements of electrons and ions. The research also demonstrated that the treatment could affect the activities of free radicals, proteins and enzymes, the permeation of biofilms, and cell growth [11]. A similar study reported that 30 mT of static magnetic field application for 15 days at 24 h per day enhanced the growth of *C. pyrenoidosa* and *Tetradesmus obliquus* by 32.8% and 31.5%, respectively, and increased protein synthesis by 44.3% [12]. Due to its convenience, low-cost, non-toxic, and non-polluting characteristics [9], MFE stimulation is being explored as a method to increase the production of microalgae biomass [13–15]. While long duration MFE could be detrimental to bioactive compound production, species-specific studies of key factors like intensity, time duration of application, etc., are needed to understand its impact on microalgal growth [16].

There are limited studies on how MFE specifically affects the microalgae *C. vulgaris*, which is a commonly found eukaryotic green microalgae species that frequently appears

in many natural and manmade freshwater and soil environments. *C. vulgaris* is known to be a source for biofuels and has the ability to decrease the amount of greenhouse gasses in the atmosphere [17]. Due to the extremely dense protein concentration (60–66%), *C. vulgaris* and other algal protein sources are being explored for human consumption and commercially used for nutritional product development [18]. With the potential use of algal pigments as natural colorants in food, beta-carotene as a potential antioxidant, and its use in the cosmetics industry, *C. vulgaris* offers an interesting perspective and a high market value [19]. *C. vulgaris* is also a good carotenoid source for potential use in foods [20]. Due to its magnetic properties and biomass, *Chlorella* cells-based magnetic biohybrid microrobot multimers have been successfully used for enhanced drug delivery [21]. *Chlorella*-based microorganisms, which have existed for thousands of years through evolution, exhibit unique structural features, which enables them to be considerably superior and cost-effective for micro/nanofabrication techniques [22]. Last but not the least, a *C. vulgaris* photobioreactor has been explored to produce oxygen and food on the lunar and other space environments [23]. An environment like that of outer space, as experienced on the International Space Station or orbits around planetary bodies, can have a critical impact on the overall growth and production of the bioactive compounds of *C. vulgaris*. The hypothesis of this study is that treatment of *C. vulgaris* with increased MFE can have a significant impact on its overall growth and bioactive compounds production. The specific objective of this study is to evaluate the effect of increased MFE on the overall growth of *C. vulgaris* in terms of optical density and the production of its bioactive compounds, beta-carotene and protein.

2. Experimental Setup and Characterization Methodology

The study was critically dependent on the capability to perform experiments in a Helmholtz cage (HHC) instrument. The state-of-the-art HHC at Old Dominion University is designed around a 150 cm triaxial square Helmholtz C-spin coil system and precision triaxial fluxgate magnetometers, and can produce a B-field of up to 7.5 Gauss (750 μT) about each axis in a volume of 30 × 30 × 30 cm^3 with a field uniformity of 99%. The magnetic field direction, intensity, and frequency can be precisely specified through the control software in real-time. The control software facilitates ambient field cancellation to create a zero-magnetic-field environment within 2–3 milli Gauss (0.2–0.3 μT). A computer-controlled rotating platform with an angular resolution of $<1^0$ can emulate the angular displacement of Earth/Mars orbiters. The HHC is also equipped with four precision 3-axis magnetometers (noise at 1 Hz is <1 nT/Hz) on a sliding platform for measuring the magnetic field with a field uniformity of 99% within the volume in which the algae specimens are placed.

2.1. Experimental Design

In this study, six treatments of *C. vulgaris* with two repetitions of each were exposed to a magnetic field of 5 Gauss (500 μT) about each axis generated in the state-of-the-art HHC (Figure 1). The treatments and the control were characterized by the duration of exposure, which was varied from 0 min to 120 min with a step increment of 20 min. The samples were placed close together on top of a cardboard stand in the center of the HHC and slowly rotated at a rate of 0.005 rev/s continuously throughout exposure. The treatments were repeated for six days in the first set of experiments (TR1) and twelve days (TR2) in the second set of experiments (Figure 2).

Figure 1. Helmholtz cage experimental setup.

Figure 2. *Chlorella vulgaris* MFE treatments for TR1 and TR2.

2.2. Algal Culture Conditions

The *C. vulgaris* microalgae culture was cultivated in a BBM medium (Bischoff HW & HC Bold, 1963) maintained at room temperature (25–27 °C). For each experiment, the cultivated specimen was transferred to twelve 250 mL conical flasks with known quantities of BBM medium for propagation. The specimens were stored at room temperature with 2500 lux illumination. The specimens thus prepared were treated with an increased MFE of 6 different time durations (20 min, 40 min, 60 min, 80 min, 100 min, and 120 min). There were also two control specimens that were not treated with the increased MFE (0 min). The specimens were treated with the increased MFE for 6 days in the first trial (TR1) and 12 days in the second trial (TR2). All samples were monitored for 21 days for growth curve and protein and beta-carotene content. The growth curve is represented by the optical density (OD at 750 nm) of the algal culture [24]. The OD method is adopted for growth monitoring to reduce biomass wastage and its ability to measure pigments (as biomass increases, pigment concentration decreases) at a particular wavelength for green algae.

2.3. Protein Extraction and Estimation

According to the Bradford method described in Reference [25], 2 mL of 0.5 M sodium hydroxide solution was added to 1 mg of dry microalgae or 10 mg (10 mL culture and centrifuge) of fresh biomass. It was then sonicated for about 30 min. The resulting extract

was then centrifuged for 15 min at a rotor speed of 7000 rpm. The resulting supernatant was then transferred to a clean chemical ware. Bradford reagent (1 mL, Sigma-Aldrich Rus, Moscow, Russia) was then added to 0.1 mL of each standard, test, and control solution. They were mixed thoroughly by inverting. This way, foam formation resulting in poor reproducibility was avoided. They were then kept at room temperature for 10 min, and the optical densities of the standard solutions and the test solution were measured with a spectrophotometer at a wavelength of 595 nm, using the control solution as a reference solution containing solvent and Bradford reagent.

2.4. Beta-Carotene Extraction and Analysis

According to the method described in Reference [26], about 20 mL of algal culture was taken and centrifuged at a rate of 7000 rpm for 10–15 min to get the biomass. Afterwards, 2 mL of absolute ethanol was added, and the samples were vortexed for about 30 s each then sonicated for 30 min at 25 °C. After this, 5 mL of KOH at 4% was added and the samples were left to stand overnight (18 h) in the absence of light in the incubator shaker. After this, 2 mL of Hexane (2:5:0.6 = Ethanol:KOH:Haxane) was added to the samples. They were again centrifuged at 7000 rpm for another 15 min to separate the hexane phase. After the hexane was separated, the OD (optical density) readings of the sample were taken with a spectrophotometer (Varian UV-Visible, Model Cary 50 CON) at 448 nm.

The estimation of total carotenoids from the biomass was carried out using the Wellburn standard curve method [27] for beta-carotene at an optical density of 448 nm with the solvent hexane. The FTIR instrument used in this study was an Agilent model, Cary 360, capable of covering the spectral range of 4000–400 cm^{-1}. The instrument was operated under a Microlab-PC FTIR software program (FTIR Essentials) run under Windows-based spectrum light. An automated flow-through transmission surface was used to handle and measure samples. The temperature of the flow cell was always at normal room temperature (25–27 °C).

3. TR1 Experimental Results

This section discusses the results of the first set of experiments TR1, where two repetitions of the propagated *C. vulgaris* specimens were treated with an increased MFE (500 μT) of 6 different time durations (20 min, 40 min, 60 min, 80 min, 100 min, and 120 min) for 6 days. There were also two control specimens that were not treated with the increased MFE (0 min).

3.1. Growth Measurements in Terms of Optical Density for TR1

The measurements taken for the overall growth in terms of optical density for the duration of the 21 days are summarized in Figure 3 and tabulated in Table 1. From the plots, it can be seen that all the samples had a steady growth rate. The growth was highest for the control sample from the initial day to the 9th day. After the 12th day, all the treated samples overtook the growth of the control treatment and showed higher growth for the later stages of the trial. At the end of the trial, treatment number 2 (40 min of MFE) showed the highest amount of growth, followed by treatment 4 (80 min of MFE), treatment 3 (60 min of MFE), treatment 1 (20 min of MFE), treatment 6 (120 min of MFE), and finally treatment 5 (100 min of MFE). Overall, it was observed at the end of the experiment that all the specimens with increased MFE treatments for 6 days showed better growth than the control sample.

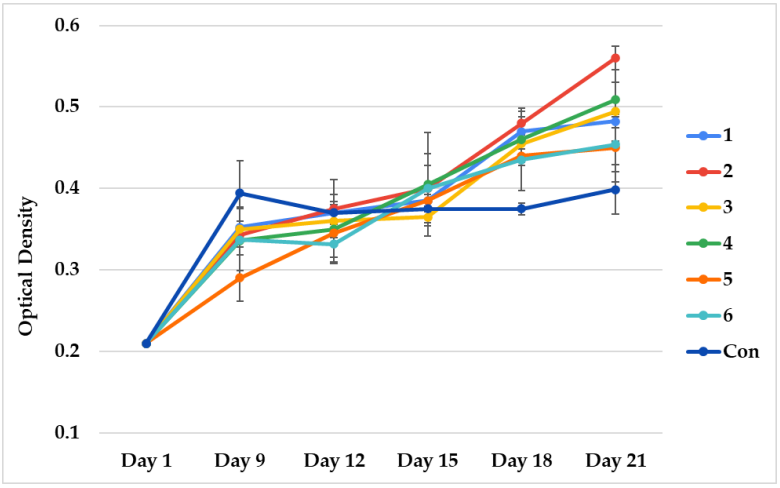

Figure 3. Growth measurements as optical density for TR1.

Table 1. Growth measurements as optical density for TR1.

	Duration	Day 1	Day 9	Day 12	Day 15	Day 18	Day 21
1	20 min	0.21 ± 0	0.352 ± 0.024	0.37 ± 0.014	0.435 ± 0.021	0.47 ± 0.028	0.482 ± 0.007
2	40 min	0.21 ± 0	0.342 ± 0	0.375 ± 0.035	0.4 ± 0.042	0.48 ± 0.014	0.55 ± 0.014
3	60 min	0.21 ± 0	0.35 ± 0.009	0.36 ± 0.014	0.365 ± 0.007	0.455 ± 0.007	0.494 ± 0.036
4	80 min	0.21 ± 0	0.336 ± 0.008	0.35 ± 0.042	0.405 ± 0.063	0.46 ± 0.028	0.509 ± 0.052
5	100 min	0.21 ± 0	0.29 ± 0.028	0.345 ± 0.035	0.385 ± 0.007	0.44 ± 0.042	0.45 ± 0.042
6	120 min	0.21 ± 0	0.337 ± 0.038	0.331 ± 0.016	0.4 ± 0.028	0.435 ± 0.007	0.454 ± 0.033
Con	Control	0.21 ± 0	0.394 ± 0.039	0.31 ± 0	0.375 ± 0.021	0.375 ± 0.007	0.398 ± 0.03

3.2. Beta-Carotene Content

The measurements taken for the beta-carotene content for the duration of the 21 days are summarized in Figure 4 and tabulated in Table 2. The beta-carotene content trends for the 6-day treatment trial show that all samples, excluding treatment 6, initially increased, peaked on the 15th day, decreased till the 18th day, and then increased afterward. On the 12th day, only treatments 6, 3, and 2 had a higher beta-carotene content than the control. On the fifteenth day, treatments 2 and 3 were the highest, followed by the control and treatments 5, 1, 4, and 6. This trend continued till the end of the trial, demonstrating that low exposure times (between 40 and 60 min) stimulated beta-carotene production better than the control, and longer treatments adversely affected beta-carotene production.

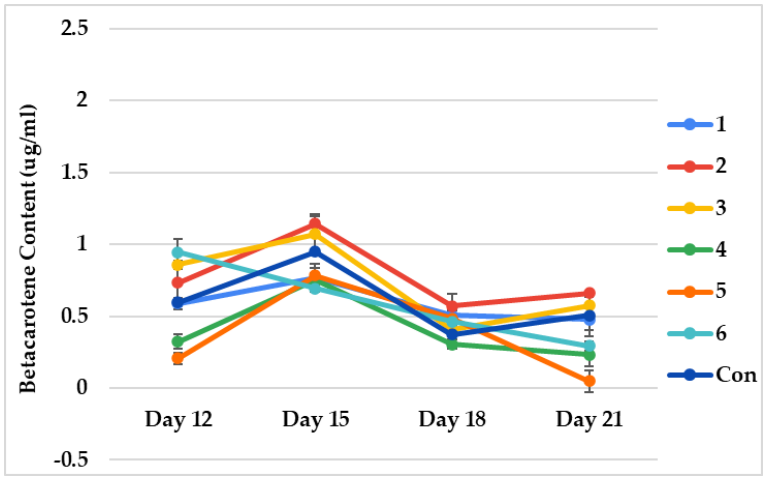

Figure 4. Beta-carotene content (µg/mL) measurements for TR1.

Table 2. Beta-carotene content (µg/mL) measurements for TR1.

	Duration	Day 12	Day 15	Day 18	Day 21
1	20 min	0.589 ± 0.04	0.766 ± 0.098	0.505 ± 0.043	0.478 ± 0.073
2	40 min	0.731 ± 0.141	1.143 ± 0.064	0.572 ± 0.083	0.659 ± 0.003
3	60 min	0.857 ± 0.03	1.071 ± 0.123	0.406 ± 0.033	0.574 ± 0.061
4	80 min	0.322 ± 0.049	0.755 ± 0.077	0.304 ± 0.03	0.232 ± 0.082
5	100 min	0.206 ± 0.04	0.783 ± 0.012	0.485 ± 0.052	0.047 ± 0.073
6	120 min	0.945 ± 0.092	0.694 ± 0.015	0.461 ± 0.006	0.293 ± 0.033
Con	Control	0.596 ± 0.03	0.949 ± 0.006	0.372 ± 0.009	0.507 ± 0.144

3.3. Protein Content

The measurements taken for the protein content for the duration of the 21 days are summarized in Figure 5 and tabulated in Table 3. The protein content in all samples strictly increased until the 15th day, peaked, and then decreased. On the 12th day, only treatment 5 contained a higher protein than the control, followed by treatments 2, 3, 1, 6, and 4. On the 15th day, treatment 6 was the highest, followed by treatments 5, 4, 3, 1, 2, and the control. At the end of the trial, the control returned to being in the middle of the treated samples. The protein production analysis shows that all the treated samples outperformed the control at the production peak, with longer treatments performing the best.

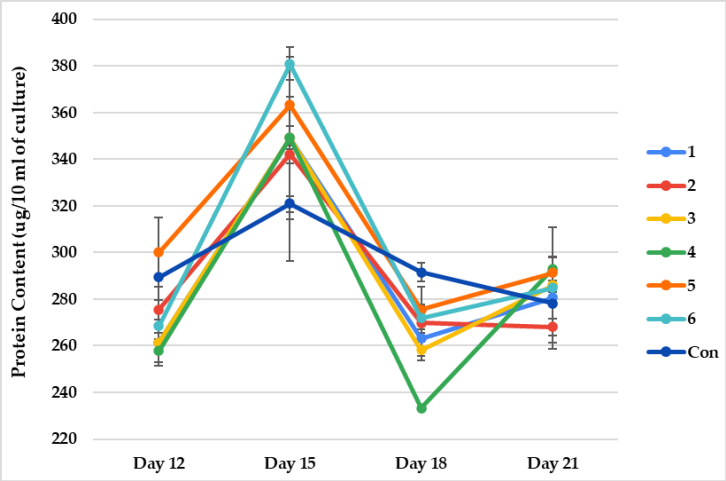

Figure 5. Protein content (µg/mL) measurements for TR1.

Table 3. Protein content (µg/mL) measurements for TR1.

	Duration	12th Day	15th Day	18th Day	21st Day
1	20 min	261.403 ± 9.924	349.122 ± 34.735	263.157 ± 7.443	280.701 ± 2.481
2	40 min	275.438 ± 9.924	342.105 ± 24.81	269.824 ± 7.939	268.07 ± 9.428
3	60 min	261.403 ± 9.924	349.122 ± 4.962	258.245 ± 4.465	285.964 ± 24.81
4	80 min	257.894 ± 4.962	349.122 ± 24.81	233.333 ± 0	292.982 ± 4.962
5	100 min	300 ± 14.886	363.157 ± 24.81	275.438 ± 9.924	291.228 ± 0.496
6	120 min	268.421 ± 0	380.701 ± 0	271.929 ± 4.962	284.912 ± 13.397
Con	Control	289.473 ± 9.924	321.052 ± 24.81	291.578 ± 3.969	278.245 ± 13.894

4. TR2 Experimental Results

This section discusses the results of the second set of experiments TR2 where two repetitions of the propagated *C. vulgaris* specimens were treated with an increased MFE (500 µT) of 6 different time durations (20 min, 40 min, 60 min, 80 min, 100 min, and 120 min) for 12 days. There were also two control specimens that were not treated with the increased MFE (0 min).

4.1. Growth in Terms of Optical Density

The measurements taken for the overall growth in terms of optical density for the duration of the 21 days are summarized in Figure 6 and tabulated in Table 4. For the growth of the second trial, undergoing 12 days of magnetic field exposure, the treated trials increased until the 12th day, decreased until the 15th day, recovered their growth rate, and increased for the rest of the trial. However, this was not the case for the control that strictly increased throughout the trial. Initially, all treatments had higher growth than the control, but this changed from the 12th day. On the 12th day, treatment 3 had the lowest growth, and the control had the second lowest. By the 15th day, all the treated samples had less growth than the control. By the end of the trial, the treated samples had recovered, but only treatments 5 and 4 were slightly higher than the control, followed by treatments 3, 1, 6, and 2. Doubling the magnetic field exposure period proved to have an adverse effect on the growth, as most treatments had a similar or lower growth than the control. In contrast, six days of exposure showed increased growth for the treated samples.

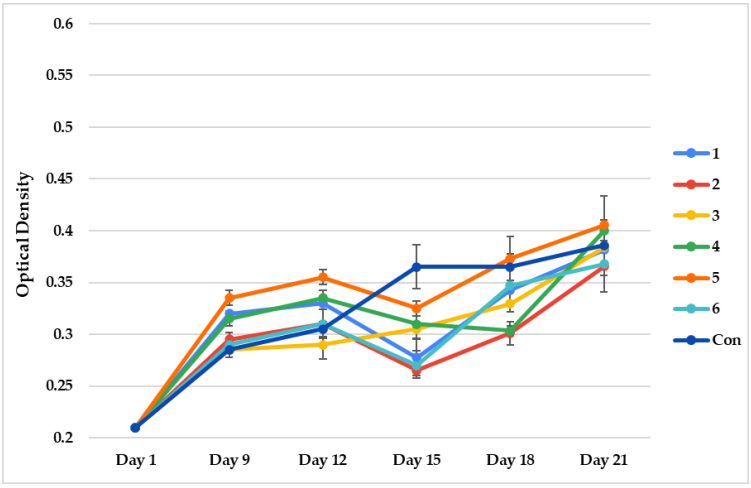

Figure 6. Growth measurements as optical density for TR2.

Table 4. Growth measurements as optical density for TR2.

	Duration	Day 1	9th Day	12th Day	15th Day	18th Day	21st Day
1	20 min	0.21 ± 0	0.32 ± 0	0.33 ± 0	0.277 ± 0.017	0.342 ± 0.02	0.381 ± 0.016
2	40 min	0.21 ± 0	0.295 ± 0.007	0.31 ± 0.014	0.265 ± 0.007	0.301 ± 0.011	0.365 ± 0.024
3	60 min	0.21 ± 0	0.285 ± 0.007	0.29 ± 0.014	0.305 ± 0.021	0.329 ± 0	0.384 ± 0.019
4	80 min	0.21 ± 0	0.315 ± 0.007	0.335 ± 0.007	0.31 ± 0.014	0.303 ± 0.004	0.4 ± 0.033
5	100 min	0.21 ± 0	0.335 ± 0.007	0.355 ± 0.007	0.325 ± 0.007	0.373 ± 0.021	0.405 ± 0.004
6	120 min	0.21 ± 0	0.29 ± 0	0.31 ± 0	0.27 ± 0	0.347 ± 0.001	0.368 ± 0.011
Con	Control	0.21 ± 0	0.285 ± 0.007	0.305 ± 0.007	0.365 ± 0.021	0.365 ± 0.012	0.386 ± 0.019

4.2. Beta-Carotene Content

The observations made for the beta-carotene content for the duration of the 21 days are summarized in Figure 7 and tabulated in Table 5. The beta-carotene content in TR2 shows a similar trend to that of TR1. It increased until the 15th day, where it peaked, then decreased till the 18th day, and finally started increasing again till the end of the trial. On the 12th day, treatments 5, 3, 4, 6, and 2 were higher than the control, leaving treatment 1 as the only one lower. On the 15th day, treatments 5, 1, 6, 4, and 2 were above the control, followed by treatment 3. Towards the end of the treatment, most treatments fell under the control, with only treatment 5 staying above. Treatment 5 performed the best, maintaining the highest beta-carotene production throughout the trial.

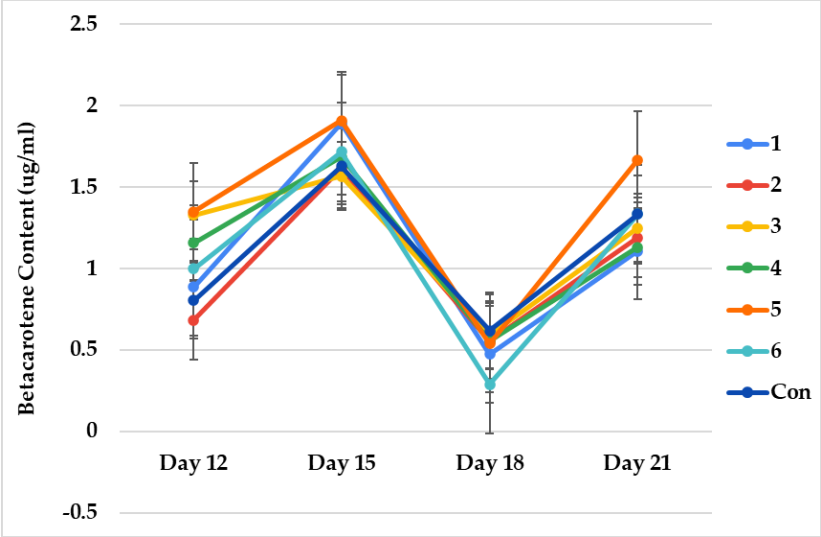

Figure 7. Beta-carotene content (µg/mL) measurements for TR2.

Table 5. Beta-carotene content (µg/mL) measurements for TR2.

	Duration	12th Day	15th Day	18th Day	21st Day
1	20 min	0.886 ± 0.157	1.89 ± 0.141	0.474 ± 0.11	1.106 ± 0.098
2	40 min	0.683 ± 0.073	1.615 ± 0.161	0.552 ± 0.08	1.189 ± 0.049
3	60 min	1.328 ± 0.375	1.568 ± 0.277	0.592 ± 0.049	1.247 ± 0.12
4	80 min	1.156 ± 0.397	1.683 ± 0.446	0.555 ± 0.113	1.13 ± 0.033
5	100 min	1.348 ± 0.003	1.908 ± 0.455	0.539 ± 0.277	1.668 ± 0.11
6	120 min	0.999 ± 0.021	1.718 ± 0.2	0.289 ± 0.206	1.335 ± 0.175
Con	Control	0.803 ± 0.046	1.629 ± 0.012	0.618 ± 0.086	1.335 ± 0.249

4.3. Protein Content

The observations made for the protein content for the duration of the 21 days are summarized in Figure 8 and tabulated in Table 6. The protein production in the treated samples had a different trend in TR2. The treated samples started with a higher protein content than the control, but the content primarily decreased until the 18th day, when it started increasing again. Initially, the shortest treatments performed the best, with treatments 2, 1, and 3 doing the best, followed by 6, 5, 4, and finally, the control. On the 15th day, which was the peak for the control, all the treated samples fell below the control. However, on the 18th day, treatments 6, 1, 5, 4, and 3 overtook the control again. At the end of the trial treatment, treatment 4 had the highest protein content, followed by the control and treatments 3, 6, 5, 1, and 2. The treated samples did much better at the beginning and the end of the trial, reaching higher protein production than control at its peak.

Table 6. Protein content (µg/mL) measurements for TR2.

	Duration	12th Day	15th Day	18th Day	21st Day
1	20 min	321.052 ± 14.886	310.526 ± 9.924	303.508 ± 19.848	298.596 ± 6.947
2	40 min	324.561 ± 19.848	303.508 ± 0	289.473 ± 0	291.929 ± 10.42
3	60 min	319.298 ± 2.481	308.07 ± 9.428	292.982 ± 4.962	309.122 ± 21.833
4	80 min	303.508 ± 0	303.508 ± 9.924	296.491 ± 0	324.561 ± 19.848
5	100 min	309.473 ± 8.435	307.017 ± 4.962	292.982 ± 24.81	300 ± 14.886
6	120 min	314.035 ± 14.886	303.508 ± 9.924	307.017 ± 4.962	307.017 ± 4.962
Con	Control	278.947 ± 14.886	310.526 ± 9.924	291.578 ± 5.954	311.228 ± 17.863

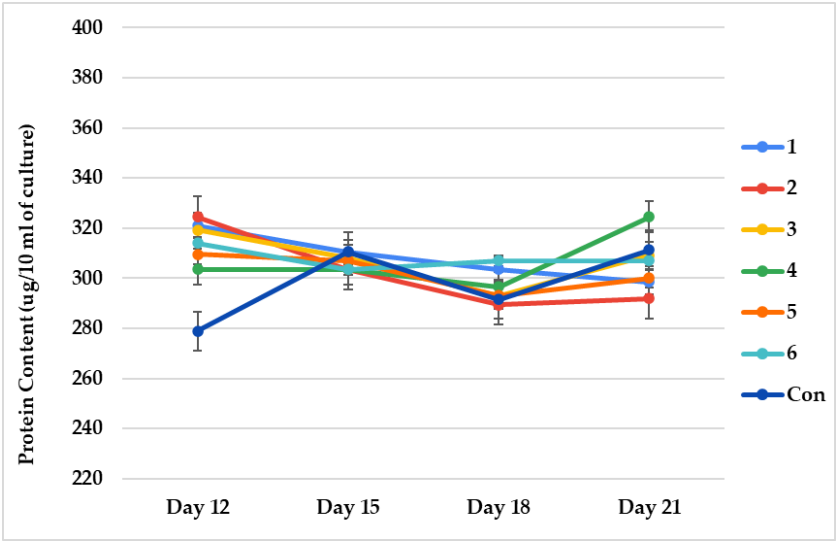

Figure 8. Protein content (μg/mL) measurements for TR2.

5. Statistical Modeling, Analysis, and Discussions

To further evaluate the time effects of the increased MFE on *C. vulgaris*, statistical modeling and analysis were performed using a longitudinal modeling approach. Specifically, the linear mixed-effects models [28] were used to identify which MFE treatments produced a significantly different trajectory of mean outcome over time compared to the control. Three different models were fitted for three different continuous outcomes, namely, optical density (growth), protein content, and beta-carotene content. Moreover, the 6-day exposure and the 12-day exposure data were modeled separately. All models were fitted using the R statistical software (https://www.r-project.org/; accessed on 29 January 2024).

5.1. Growth in Terms of Optical Density (TR1)

For the optical density (growth) outcome, the model identified significant interaction between time and MFE durations. All the six MFE durations have a significantly different (higher) rate of change in optical density with time when compared to the control. The significant interaction effects between time and MFE durations are tabulated in Table 7 and summarized in Figure 9.

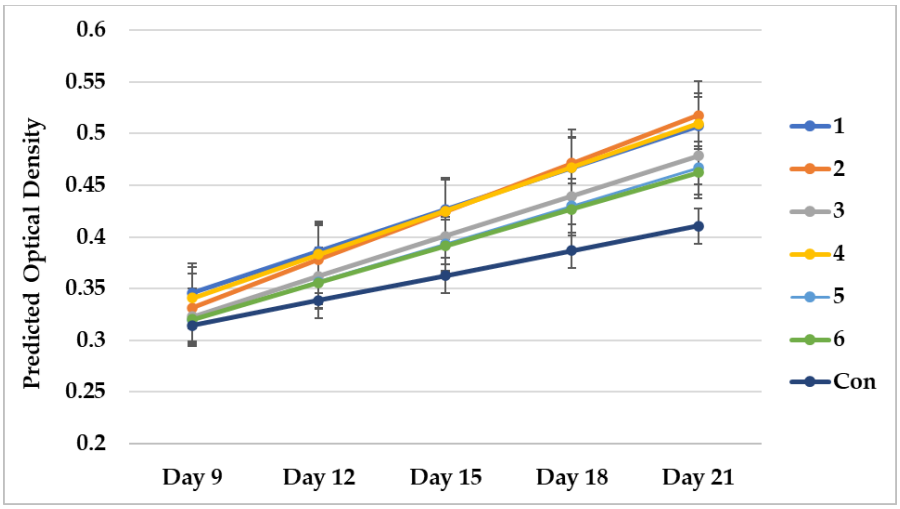

Figure 9. Interaction plot of time and MFE treatments for optical density (TR1).

Table 7. Interaction effects between time and MFE treatments for optical density (TR1).

	Duration	Effect Estimate (Standard Error)	*p*-Value *
1	20 min	5.4×10^{-3} (1.7×10^{-3})	0.002
2	40 min	7.5×10^{-3} (1.7×10^{-3})	<0.001
3	60 min	4.9×10^{-3} (1.7×10^{-3})	0.005
4	80 min	6.0×10^{-3} (1.7×10^{-3})	0.001
5	100 min	4.2×10^{-3} (1.7×10^{-3})	0.015
6	120 min	3.8×10^{-3} (1.7×10^{-3})	0.028

* All the above *p*-values are significant at 5% level of significance.

5.2. Beta-Carotene Content (TR1)

For the beta-carotene content outcome, the model did not find any significantly different rate of change over time for the MFE durations compared to the control. Figure 10 shows the predicted beta-carotene trajectories for the various MFE treatments although they did not turn out to be statistically significant.

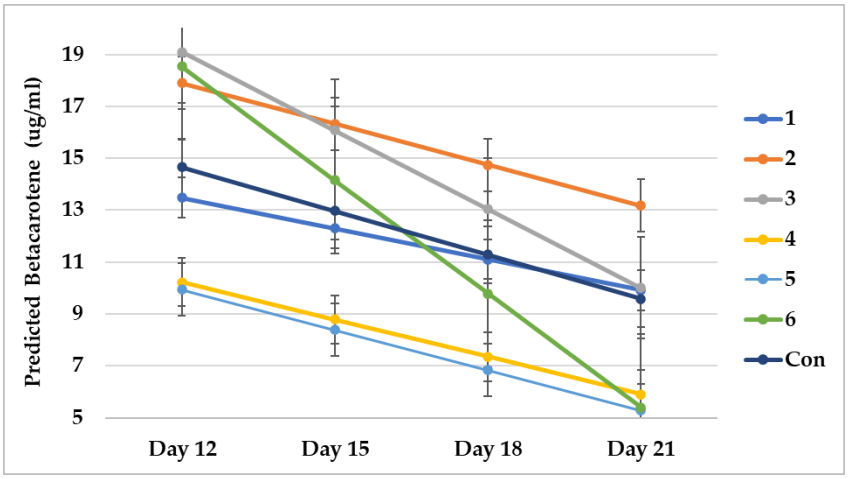

Figure 10. Interaction plot of time and MFE treatments for beta-carotene (TR1).

5.3. Protein Content (TR1)

For the protein content outcome, the model did not find any significantly different rate of change over time for the MFE durations compared to the control. Figure 11 shows the predicted protein content trajectories for the various MFE treatments although they did not turn out to be statistically significant.

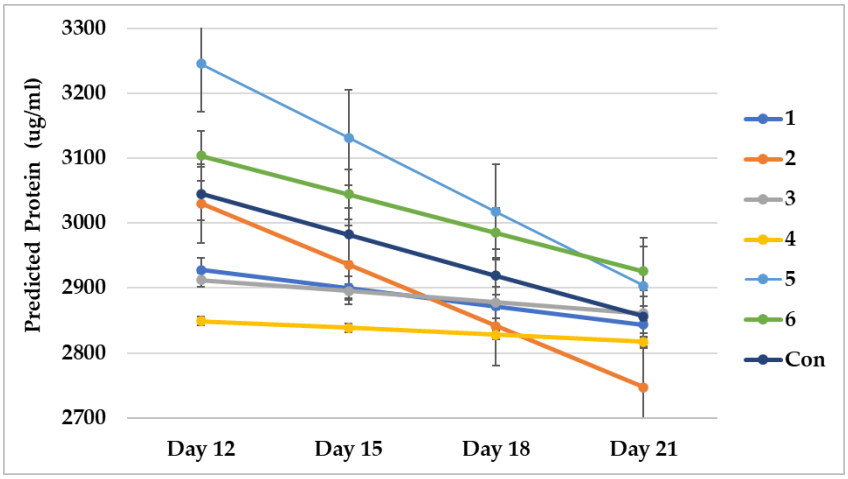

Figure 11. Interaction plot of time and MFE treatments for protein (TR1).

5.4. Growth in Terms of Optical Density (TR2)

For the optical density outcome, the model did not find any significantly different rate of change over time for the MFE durations compared to the control. Figure 12 shows the predicted optical density trajectories for the various MFE treatments although they did not turn out to be statistically significant.

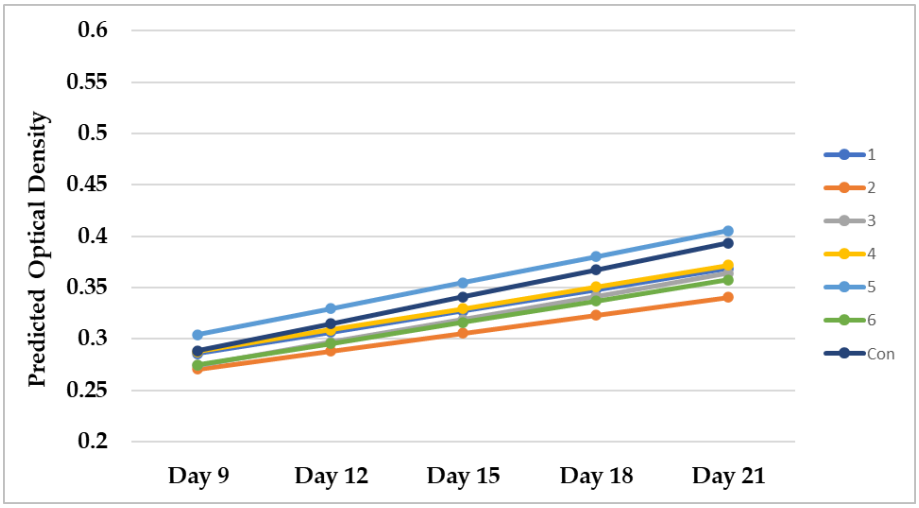

Figure 12. Interaction plot of time and MFE treatments for optical density (TR2).

5.5. Beta-Carotene Content (TR2)

For the beta-carotene content outcome, the model did not find any significantly different rate of change over time for the MFE durations compared to the control. The figure below shows the predicted beta-carotene trajectories for different MFE durations although they did not turn out to be statistically significant.

5.6. Protein Content (TR2)

For the protein content outcome, the model identified significant interaction between time and some of the MFE durations, which is different from the TR1 results on the protein content. The increased MFE durations that produced a significantly different rate of change with time, compared to the control, were the 20-min, 40-min, 60-min, and 100-min exposures. The significant interaction effects between time and MFE durations are tabulated in Table 8 and summarized in Figure 13.

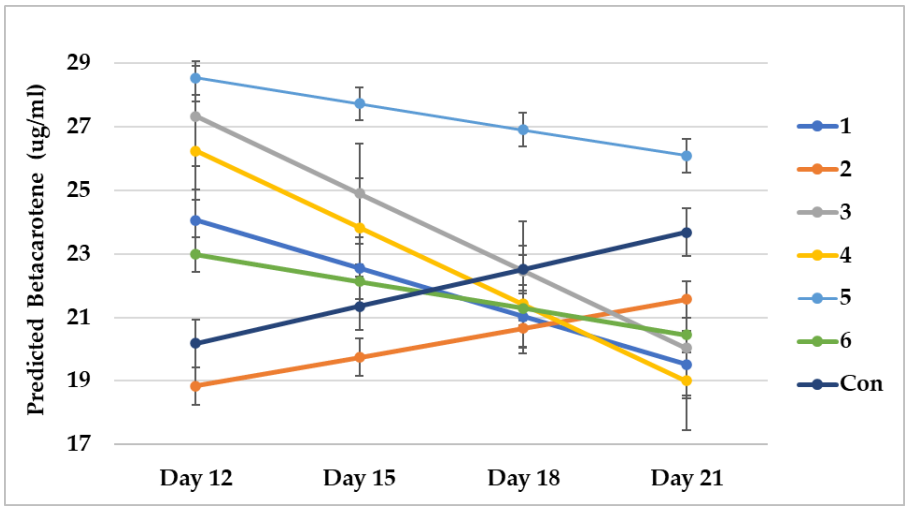

Figure 13. Interaction plot of time and MFE treatments for beta-carotene (TR2).

Table 8. Interaction effects between time and MFE treatments for protein (TR2).

	Duration	Effect Estimate (Standard Error)	*p*-Value
1	20 min	−50.760 (18.973)	0.011
2	40 min	−63.275 (18.973)	0.002
3	60 min	−41.170 (18.973)	0.036
4	80 min	−7.251 (18.973)	0.704
5	100 min	−40.117 (18.973)	0.041
6	120 min	−31.813 (18.973)	0.101

From Table 8 we see that the effect estimates of interactions are negative, implying that the protein content tends to decrease at a faster rate under most of the increased MFEs compared to the control. The *p*-values are significant (<0.05) for the 20-min, 40-min, 60-min, and 100-min exposure durations. The faster decrease in the protein content under these four MFE durations are also evident from the plot shown in Figure 14.

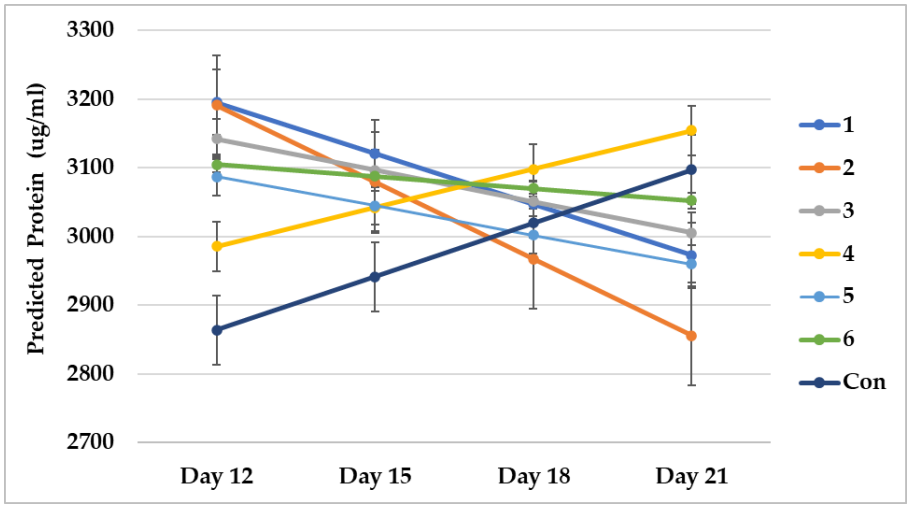

Figure 14. Interaction plot of time and MFE treatments for protein (TR2).

5.7. Discussion

In TR1, the treated samples demonstrated a higher growth rate than the control. The growth was highest on the 21st day of treatment for an MFE duration of 40 min and was found to be 38% higher than the control. The protein content was highest on the 15th day of treatment for an MFE duration of 120 min, which was 15.6% higher than the control. The beta-carotene content was also highest on the 15th day of treatment for an MFE duration of 40 min, which was 20.4% higher than the control. In TR2, the results were less promising, possibly due to the longer period of MFE, but still showed higher production than the control. The protein content was highest on the 21st day of treatment for an MFE duration of 80 min and found to be 4.28% higher than the control. The beta-carotene content was highest on the 15th day of treatment for an MFE duration of 100 min and found to be 17.1% higher than the control. The growth was highest on the 21st day of treatment for an MFE duration of 100 min, which was 5% higher than the control. Overall, TR1 exhibited significantly higher production compared to TR2; however, the TR2 treatments exhibited higher production compared to the control.

Statistically, the model of TR1 identified significant interaction between time and MFE durations. All the six increased MFE durations had significantly different (higher) rates of change in optical density with time when compared to the control. Similarly, for the protein content outcome in TR2, the model identified a significant interaction between time and some of the MFE durations, which is different from the TR1 results on the protein content. The MFE durations that produced significantly different rates of change with time, compared to the control, were the 20-min, 40-min, 60-min, and 100-min exposures.

6. Conclusions

It is well established that exposure to magnetic fields not characteristic of Earth can have a significant effect on biological systems [13,29,30]. Physiological stress, such as that induced by an MFE of an order of magnitude higher than that experienced on the surface of Earth, can stimulate the antioxidant response and growth in microalgae such as *C. vulgaris* [29,30] and *Dunaliella salina* [31]. Due to their higher yield and shorter cultivation time compared to plants, microalgae as an alternative source are gaining popularity in the industrial production of bioactive compounds [32]. *Haematococcus pluvialis*, *Chlorella* sp., and *Spirulina* sp. are considered among the microalgae of highest commercial value [33,34]. Microalgae such as *C. vulgaris* synthesize a variety of carotenoids including beta-carotene and are a rich source of natural beta-carotene. It is well known that beta-carotene is widely used in the biomedical field, but the beta-carotene products on the market are mainly synthetic. The production of natural beta-carotene from sources like *C. vulgaris* can be positively influenced through MFE stimulation with limited or no environmental impact. However, it is critical to parametrically study the intensity and exposure time of the MFE as influencing factors [14]. There are limited studies that report on the production of protein and beta-carotene content due to the MFE stimulation of *C. vulgaris.* This study contributes to the fundamental understanding of the effect of increased magnetic field exposure on the growth and production of *C. vulgaris*. It was largely observed that the increased MFE had a significant impact on the overall growth and to a lesser extent on the protein and beta-carotene production.

Author Contributions: Conceptualization, S.A.; methodology, S.A., S.R., S.S. and S.K. (Sanghamitra Khandual); formal analysis, S.D.; investigation, S.A., S.R., S.S. and S.K. (Sanghamitra Khandual); data curation, S.R., S.S. and S.K. (Sanghamitra Khandual); writing—original draft preparation, S.R., S.S. and S.K. (Sanghamitra Khandual); writing—review and editing, S.A.; visualization, S.R., S.S. and S.K. (Sanghamitra Khandual); supervision, S.K. (Sandeep Kumar); project administration, S.K. (Sandeep Kumar); funding acquisition, S.A. All authors have read and agreed to the published version of the manuscript.

Funding: This research was supported by the National Science Foundation (Agency Tracking Number: 1949952, Project Title: Research Initiation Award: Magnetic Field Mapping of Pico/Nano/Micro-Satellites to Facilitate Refinement of their Guidance/Navigation Systems and Magnetic Cleanliness).

Data Availability Statement: The original contributions presented in the study are included in the article, further inquiries can be directed to the corresponding author.

Acknowledgments: The authors would like to acknowledge the support of the National Science Foundation, and Old Dominion University for providing a platform for this research and supporting it. The authors would also like to acknowledge Virginia Space Grant Consortium for their motivation to conduct space research and engage students.

Conflicts of Interest: The authors declare no conflicts of interest. The funders had no role in the design of the study; in the collection, analyses, or interpretation of data; in the writing of the manuscript; or in the decision to publish the results.

References

1. Connerney, J.E.P. Planetary Magnetism. In *Planets and Moons*, 1st ed.; Spohn, T., Schubert, G., Eds.; Elsevier B.V.: Amsterdam, The Netherlands, 2009; Volume 10, pp. 243–280.
2. Gaidos, E.; Conrad, C.P.; Manga, M.; Hernlund, J. Thermodynamic limits on magnetodynamos in rocky exoplanets. *Astrophys. J.* **2010**, *718*, 596–607. [CrossRef]
3. Jones, C.A. Planetary magnetic fields and fluid dynamos. *Annu. Rev. Fluid Mech.* **2011**, *43*, 583–614. [CrossRef]
4. Bagenal, F. Planetary Magnetospheres. In *Solar System Magnetic Fields*, 1st ed.; Priest, E.R., Ed.; D. Reidel Publishing Company: Dordrecht, The Netherlands, 1985; Volume 28, pp. 224–254.
5. Langlais, B.; Lesur, V.; Purucker, M.E.; Connerney, J.E.P.; Mandea, M. Crustal magnetic fields of terrestrial planets. *Space Sci. Rev.* **2010**, *152*, 223–249. [CrossRef]

6. Zhang, T. A Space Charging Model for the Origin of Planets' Magnetic Fields. *Prog. Phys.* **2019**, *15*, 92–100.
7. Hulot, G.; Finlay, C.C.; Constable, C.G.; Olsen, N.; Mandea, M. The magnetic field of planet earth. *Space Sci. Rev.* **2010**, *152*, 159–222. [CrossRef]
8. Serrano, G.; Miranda- Ostojic, C.; Ferrada, P.; Wulff-Zotelle, C.; Maureira, A.; Fuentealba, E.; Gallardo, K.; Zapata, M.; Rivas, M. Response to Static Magnetic Field-Induced Stress in *Scenedesmus obliquus* and *Nannochloropsis gaditana*. *Mar. Drugs* **2021**, *19*, 527. [CrossRef] [PubMed]
9. Tu, R.; Jin, W.; Xi, T.; Yang, Q.; Han, S.F.; Abomohra, A.E.F. Effect of static magnetic field on the oxygen production of Scenedesmus obliquus cultivated in municipal wastewater. *Water Res.* **2015**, *86*, 132–138. [CrossRef] [PubMed]
10. Small, D.P.; Hüner, N.P.; Wan, W. Effect of static magnetic fields on the growth, photosynthesis and ultrastructure of *Chlorella kessleri* microalgae. *Bioelectromagnetics* **2012**, *33*, 298–308. [CrossRef] [PubMed]
11. Yang, G.J.; Wang, J.; Mei, Y.; Luan, Z. Effect of magnetic field on protein and oxygen production of *Chorella vulgaris*. *Math. Phys. Fish. Sci.* **2011**, *9*, 116–126.
12. Li, C.; Hu, Z.; Gao, Y.; Ma, Y.; Pan, X.; Li, X.; Liu, S.; Chu, B. Bioeffects of static magnetic fields on the growth and metabolites of *C. pyrenoidosa* and *T. obliquus*. *J. Biotechnol.* **2022**, *351*, 1–8. [CrossRef]
13. Hunt, R.W.; Zavalin, A.; Bhatnagar, S.; Chinnasamy, K.C. Electromagnetic biostimulation of living cultures for biotechnology, biofuel and bioenergy applications. *Int. J. Mol. Sci.* **2009**, *10*, 4719–4722. [CrossRef]
14. Deamici, K.M.; Cardias, B.B.; Costa, J.A.V.; Santos, L.O. Static magnetic fields in culture of *Chlorella fusca*: Bioeffects on growth and biomass composition. *Process. Biochem.* **2016**, *51*, 912–916. [CrossRef]
15. Bauer, L.M.; Costa, J.A.V.; Rosa, A.P.C.; Santos, L.O. Growth stimulation and synthesis of lipids, pigments and antioxidants with magnetic fields in *Chlorella kessleri* cultivations. *Bioresour. Technol.* **2017**, *244*, 1425–1432. [CrossRef] [PubMed]
16. Rai, S. Causes and mechanism (s) of ner bioeffects. *Electro. Magnetobiol.* **1997**, *16*, 59–67. [CrossRef]
17. Wirth, R.; Pap, B.; Böjti, T.; Shetty, P.; Lakatos, G.; Bagi, Z.; Kovács, K.L.; Maróti, G. *Chlorella vulgaris* and its Phycosphere in Wastewater: Microalgae-Bacteria Interactions During Nutrient Removal. *Front. Bioeng. Biotechnol.* **2020**, *8*, 557–572. [CrossRef] [PubMed]
18. Canelli, G.; Tarnutzer, C.; Carpine, R.; Neutsch, L.; Bolten, C.J.; Dionisi, F.; Mathys, A. Biochemical and nutritional evaluation of *Chlorella* and *Auxenochlorella* biomasses relevant for food application. *Front. Nutr.* **2020**, *7*, 565996. [CrossRef] [PubMed]
19. Damergi, E.; Schwitzguébel, J.P.; Refardt, D.; Sharma, S.; Holliger, C.; Ludwig, C. Extraction of carotenoids from *Chlorella vulgaris* using green solvents and syngas production from residual biomass. *Algal Res.* **2017**, *25*, 488–495. [CrossRef]
20. Gille, A.; Trautmann, A.; Posten, C.; Briviba, K. Bioaccessibility of carotenoids from *Chlorella vulgaris* and *Chlamydo-monas reinhardtii*. *Int. J. Food Sci. Nutr.* **2016**, *67*, 507–513. [CrossRef] [PubMed]
21. Gong, D.; Celi, N.; Zhang, D.; Cai, J. Magnetic Biohybrid Microrobot Multimers Based on *Chlorella* Cells for Enhanced Targeted Drug Delivery. *ACS Appl. Mater. Interfaces* **2022**, *14*, 6320–6330. [CrossRef]
22. Gong, D.; Sun, L.; Li, X.; Zhang, W.; Zhang, D.; Cai, J. Micro/Nanofabrication, Assembly, and Actuation Based on Microorganisms: Recent Advances and Perspectives. *Small Struct.* **2023**, *4*, 2200356. [CrossRef]
23. Detrell, G. *Chlorella vulgaris* photobioreactor for oxygen and food production on a Moon base—Potential and challenges. *Front. Astron. Space Sci.* **2021**, *8*, 700579. [CrossRef]
24. Young, E.B.; Reed, L.; Berges, J.A. Growth parameters and responses of green algae across a gradient of phototrophic, mixotrophic and heterotrophic conditions. *PeerJ* **2022**, *10*, 13776. [CrossRef]
25. Andreeva, A.; Budenkova, E.; Babich, O.; Sukhikh, S.; Ulrikh, E.; Ivanova, S.; Prosekov, A.; Dolganyuk, V. Production, Purification, and Study of the Amino Acid Composition of Microalgae Proteins. *Molecules* **2021**, *26*, 2767. [CrossRef] [PubMed]
26. Hajare, R.; Ray, A.; Shreya, T.C.; Avadhani, M.N.; Selvaraj, I.C. Extraction and quantification of antioxidant lutein from various plant sources. *Int. J. Pharm. Sci. Rev. Res.* **2013**, *22*, 152–157.
27. Wellburn, A.R. The Spectral Determination of Chlorophylls a and b, as well as Total Carotenoids, Using Various Solvents with Spectrophotometers of Different Resolution. *J. Plant Physiol.* **1994**, *144*, 307–313. [CrossRef]
28. Bates, D.; Mächler, M.; Bolker, B.; Walker, S. Fitting Linear Mixed-Effects Models Using lme4. *J. Stat. Softw.* **2015**, *67*, 1–48. [CrossRef]
29. Wang, H.Y.; Zeng, X.B.; Guo, S.Y.; Li, Z.T. Effects of magnetic field on the antioxidant defense system of recirculation-cultured *Chlorella vulgaris*. *Bioelectromagnetics* **2008**, *29*, 39–46. [CrossRef] [PubMed]
30. Luo, X.; Zhang, H.; Li, Q.; Zhang, J. Effects of static magnetic field on *Chlorella vulgaris*: Growth and extracellular polysaccharide (EPS) production. *J. Appl. Phycol.* **2020**, *32*, 2819–2828. [CrossRef]
31. Yamaoka, Y.; Takimura, O.; Fuse, H.; Kaminura, K. Effect of magnetism on growth of *Dunaliella salina*. *Res. Photo-Synth.* **1992**, *3*, 87–90.
32. Barkia, I.; Saari, N.; Manning, S.R. Microalgae for high-value products towards human health and nutrition. *Mar. Drugs* **2019**, *17*, 304. [CrossRef]

33. Kratzer, R.; Murkovic, M. Food Ingredients and Nutraceuticals from Microalgae: Main Product Classes and Biotechnological Production. *Foods* **2021**, *10*, 1626. [CrossRef] [PubMed]
34. Vieira, M.V.; Pastrana, L.M.; Fuciños, P. Microalgae Encapsulation Systems for Food, Pharmaceutical and Cosmetics Applications. *Mar. Drugs* **2020**, *18*, 644. [CrossRef] [PubMed]